

Phonon bottleneck in GaAs/Al_xGa_{1-x}As quantum dots

Y. C. Chang, A. J. Robson, S. Harrison, Q. D. Zhuang, and M. Hayne^a
Department of Physics, Lancaster University, Lancaster, LA1 4YB, UK

(Received 27 March 2015; accepted 5 June 2015; published online 22 June 2015)

We report low-temperature photoluminescence measurements on highly-uniform GaAs/Al_xGa_{1-x}As quantum dots grown by droplet epitaxy. Recombination between confined electrons and holes bound to carbon acceptors in the dots allow us to determine the energies of the confined states in the system, as confirmed by effective mass calculations. The presence of acceptor-bound holes in the quantum dots gives rise to a striking observation of the phonon-bottleneck effect. © 2015 Author(s). All article content, except where otherwise noted, is licensed under a Creative Commons Attribution 3.0 Unported License. [<http://dx.doi.org/10.1063/1.4922950>]

Charge carrier relaxation is known to be a very rapid process in bulk and two-dimensional semiconductors, where there is a continuum of states that allow phonon emission whilst conserving energy and momentum. In contrast, the discrete energy levels in quantum dots (QDs) leads to the expectation that single-particle carrier relaxation should be very slow, unless the separation between confined states is commensurate with the longitudinal optical (LO) phonon energy (36 meV in GaAs).¹ The so-called ‘phonon bottleneck’ was thus predicted to be a severe limitation to the performance of QD-based devices,² but it has turned out to be remarkably conspicuous by its absence, and it was 10 years before it was observed, using time-resolved differential transmission spectroscopy.³ It is now known that efficient carrier relaxation proceeds as a multi-particle process⁴ involving electron and hole.⁵ However, remove the hole and the phonon bottleneck appears.³ Here we report conventional photoluminescence (PL) measurements on a large ensemble of highly-uniform GaAs/Al_xGa_{1-x}As QDs grown by droplet epitaxy.⁶ We show that at low temperature the PL is dominated by recombination of confined electrons with acceptor-bound holes (e-A⁰). Trapping of holes by carbon impurities disables multi-particle processes, turning on the phonon bottleneck, and preventing relaxation of electrons to lower confined states: e-A⁰ recombination from the highest electron state ($n = 4$) is 30 times brighter than that from the ground state ($n = 1$). Raising the temperature generates free holes, strongly increasing the confined-electron to confined-hole recombination intensity, whilst also turning off the phonon bottleneck, and allowing electrons to relax to lower energy states.

Droplet epitaxy is becoming increasingly popular for the fabrication of semiconductor nanostructures due to its broad applicability: it can be used for both lattice-matched and lattice-mismatched systems and produces a wide variety of morphologies.⁷⁻¹⁰ GaAs/Al_xGa_{1-x}As QDs are particularly appealing because both materials are extremely well understood and the dots are strain-free, making it a model system for the study of zero-dimensional physics. In droplet epitaxy, metallic Ga droplets are first formed on the surface of the wafer in the absence of As flux, and are subsequently crystallized through exposure to As flux for the formation of GaAs QDs. Ga droplets are usually formed at low temperature (~ 300 °C) in order to maintain their original morphology.¹¹ However, such low temperatures often cause degradation of crystalline and optical quality during the deposition of the Al_xGa_{1-x}As capping layer.^{12,13} Moreover, the low-temperature growth also strongly influences the formation of GaAs, and increases the incorporation of carbon impurities.¹⁴ This, as we shall show, can be exploited.

Recombination between confined electrons and acceptor-bound holes has a number of advantages for the study of novel physical phenomena in semiconductor nanostructures. Since

^ae-mail: m.hayne@lancaster.ac.uk



the bound-hole energy is well defined, PL is a direct measurement of the energy spectrum of the electronic states, and localization of the hole also relaxes \mathbf{k} -conservation rules, such that the entire electronic density of states can be investigated.^{15,16} Furthermore, in the initial state, i.e. prior to recombination, the acceptor is occupied by a photo-excited hole and is neutral, so provides only a very small perturbation to the electronic states of the system under investigation. Electron to neutral acceptor recombination was used very successfully by Kukushkin and co-workers to probe the physics of two-dimensional (2D) electron systems,¹⁷ leading to optical investigation of Landau levels,^{15,16,18} Shubnikov-de Haas oscillations,¹⁹ the fractional quantum Hall effect^{20,21} and Wigner crystallization.^{22,23} However, despite the intense interest in the physics and applications of low-dimensional semiconductors which continues to the present day, there is, to our knowledge, no equivalent experimental work involving zero-dimensional structures.²⁴

The samples were grown by solid-source molecular beam epitaxy on GaAs substrates. After the deposition of a GaAs buffer layer, a 100-period 28-Å/28-Å GaAs/AlAs superlattice was grown, followed by a 50-nm, $\text{Al}_{0.29}\text{Ga}_{0.71}\text{As}$ layer. The Ga droplets were then deposited and crystallized using a variation on standard techniques for QD formation by droplet epitaxy. The dots were capped by a further 50-nm $\text{Al}_{0.29}\text{Ga}_{0.71}\text{As}$ layer and another superlattice to form a dot-in-a-well (DWELL) structure, where the superlattice forms the barriers of the well (Fig. 1). The sample was completed with a final $\text{Al}_{0.29}\text{Ga}_{0.71}\text{As}$ layer and the formation of surface GaAs QDs, the morphology of which was investigated by atomic force microscopy (AFM). PL experiments were carried out at temperatures between 4 and 300 K in an Oxford Instruments flow cryostat, using multimode optical fibers to transmit 532-nm laser light to the sample and to collect the PL, which was analysed by a spectrometer and electron-multiplying charge-coupled device.

Fig. 2(a) shows a typical low-temperature spectrum at an incident laser power of 5.43 mW. Five peaks can be seen, labelled Peak 1 through to Peak 5, going from low to high energy. Peak 1 to Peak 4 are attributed to recombination of electrons in confined states, $n = 1$ to 4, with a hole bound to a carbon acceptor (electron to neutral acceptor, $e\text{-A}^0$), whilst Peak 5 is assigned to recombination of electrons in the $n = 4$ state with heavy holes (hh) in the ground state of the QD. At longer wavelengths an $e\text{-A}^0$ peak is observed ~ 30 meV below the bulk GaAs peak [inset to Fig. 2(a)], confirming the presence of carbon in the sample.²⁵ The average full-width at half maximum of Peak 1 to Peak 3 (from 2 to 21 K) is 10 meV, which is comparable to or lower than the best values reported in the literature for GaAs/ $\text{Al}_x\text{Ga}_{1-x}\text{As}$ QDs,^{26–28} indicating highly uniform dots.

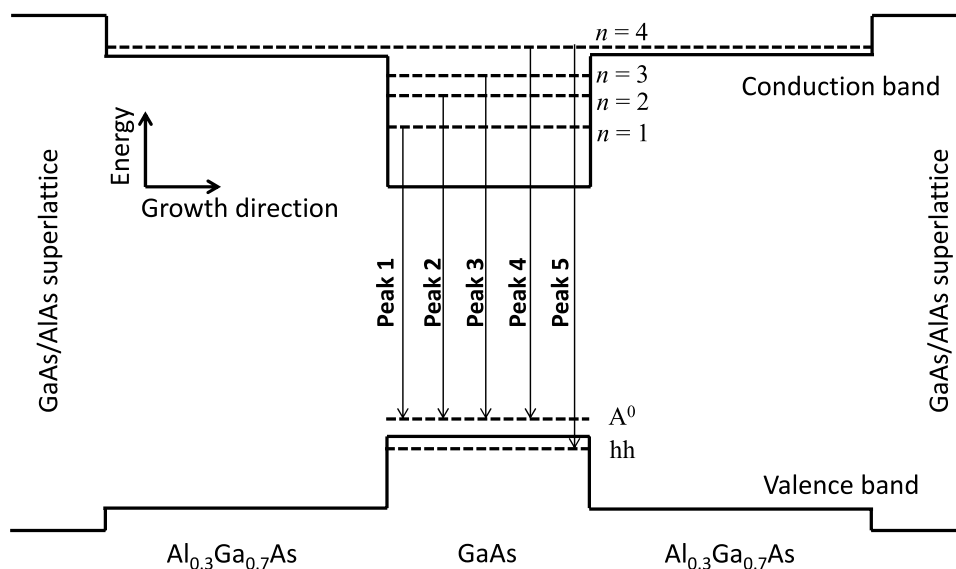


FIG. 1. Schematic band-diagram of the active layers of sample used to model the experimental results (not to scale). The horizontal lines show the energies of the confined electron and heavy-hole levels, and the carbon acceptor (A^0). The transitions observed in the PL experiment are indicated as Peak 1, Peak 2 etc.

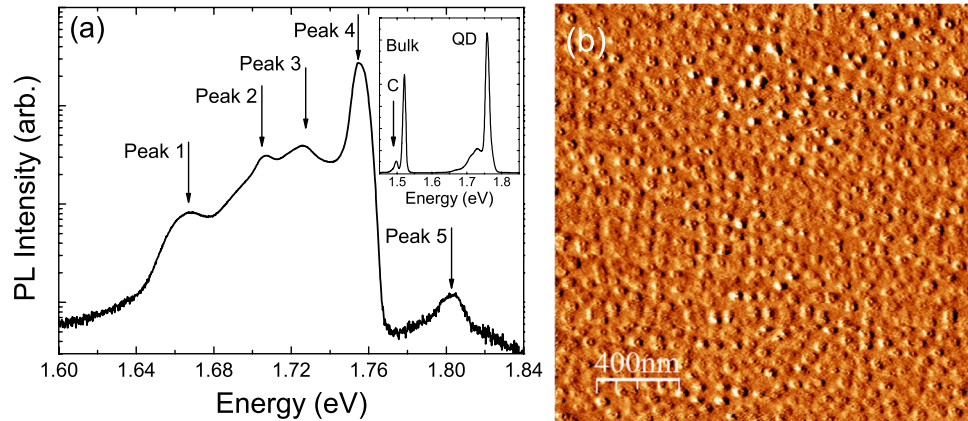


FIG. 2. (a) Low temperature (4 K) spectrum of the GaAs/Al_xGa_{1-x}As luminescence (logarithmic intensity scale). Peaks 1 to 4 are confined-electron to neutral-acceptor transitions ($e-A^0$), while Peak 5 is the result of band-to-band recombination between electrons in the Al_xGa_{1-x}As quantum well and heavy holes (hh) confined to the dots. The wider spectrum in the inset (linear intensity scale) also shows the bulk GaAs recombination at lower energy. The peak labelled C is attributed to $e-A^0$ recombination in the bulk. (b) $2 \times 2 \mu\text{m}$ AFM derivative image of the surface of the sample.

The high uniformity is demonstrated by the AFM image of surface dots shown in Fig. 2(b). The dots have a tendency towards a volcano-like morphology, i.e. with a small central recess. The average height and base diameter are $2.3 \pm 0.5 \text{ nm}$ and $48 \pm 5 \text{ nm}$ respectively, while the areal density is $2.0 \pm 0.1 \times 10^{10} \text{ cm}^{-2}$. Each of the PL peaks Peak 1 to Peak 4 represent recombination of confined electrons with the same localized state (a hole bound to an acceptor), so their separation is a direct measurement of the separation of the confined electron energy levels in the system. Indeed, the energies of the confined electron states may be found by subtracting the GaAs band gap and the carbon acceptor binding energy from the PL energies. Table I lists the energies of the confined electron states, derived from the average of 20 measurements of the PL energy between 1.7 and 21 K (Fig. 3).

In order to confirm our assignment of the PL peaks, the confined electron states in the system were calculated using an effective mass model in which the Γ -valley electron effective mass m_e^* is given in terms of band parameters by²⁹

$$\frac{m_0}{m_e^*} = (1 + 2F) + \frac{E_p(E_g + \frac{2\Delta_{SO}}{3})}{E_g(E_g + \Delta_{SO})}, \quad (1)$$

where m_0 is the free electron mass, F is Kane parameter, Δ_{SO} is spin-orbit splitting parameter, E_p is a band parameter associated with carrier momentum and E_g is the band-gap energy. The band parameters for GaAs and Al_xGa_{1-x}As were obtained from Ref. 29 using Vergard's rule for the Al_xGa_{1-x}As with an Al fraction, x , of 0.30. The conduction band offset between GaAs and Al_{0.29}Ga_{0.71}As was taken to be 62% of the difference in their band gaps.¹ The GaAs/Al_xGa_{1-x}As system is unstrained,

TABLE I. Confined electron to neutral acceptor transition energies and electron confinement energies. The experimental confinement energies are obtained by subtracting a temperature-dependent value for the GaAs band gap and the carbon acceptor binding energy of -30 meV . Details of how the theoretical values were calculated are given in the text.

| PL peak (electron level) | PL peak energy (meV) | Confinement energy | |
|--------------------------|----------------------|--------------------|--------------|
| | | Experiment (meV) | Theory (meV) |
| Peak 1 (e1) | 1668.2 ± 0.6 | 177.8 ± 0.5 | 176.5 |
| Peak 2 (e2) | 1710 ± 2 | 219 ± 2 | 206.9 |
| Peak 3 (e3) | 1726 ± 1 | 235.1 ± 0.8 | 241.6 |
| Peak 4 (e4) | 1756 ± 1 | 266 ± 1 | 267.0 |

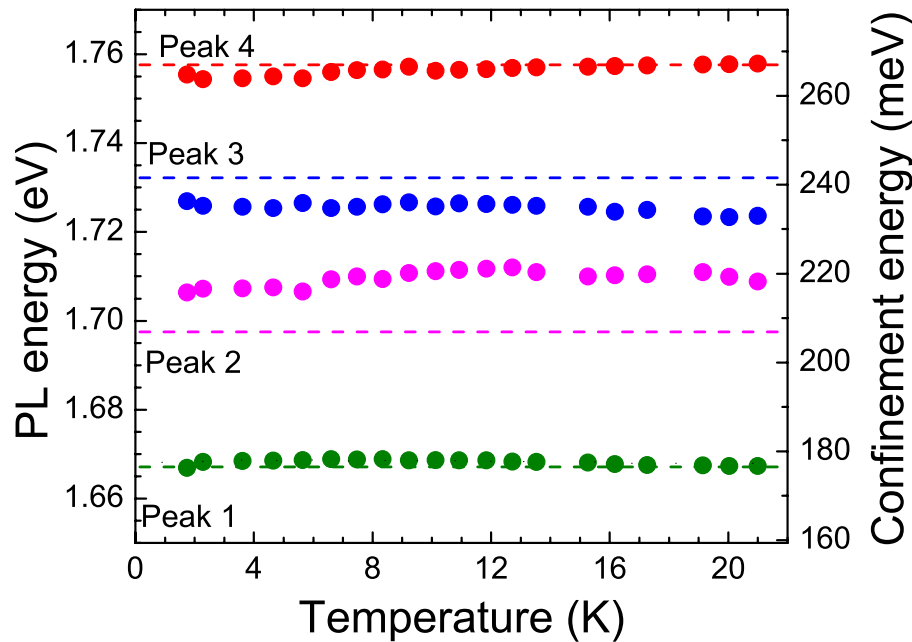


FIG. 3. Low-temperature confined electron to neutral acceptor transition energies (left axis). The right axis gives the corresponding confinement energies, which are derived by subtracting $(1520 - 30)$ meV. The dotted lines show the calculated confinement energies.

so it is expected that buried GaAs dots will be the same as surface dots.³⁰ However, for simplicity the QDs were assumed to be elliptical in cross section, with a diameter of 50 nm.³¹ The best agreement with the confinement energies was found with a dot height of 2.17 nm, which is within uncertainty of the experimental value. The $\text{Al}_x\text{Ga}_{1-x}\text{As}$ thickness was taken from cross-sectional AFM,³² and the mini-band energies in the GaAs/AlAs superlattice bounding the $\text{Al}_x\text{Ga}_{1-x}\text{As}$ were taken to be infinite. The calculated confinement energies are compared to the experimental values in Table I. The theoretical values for the energy states agree within 3% of the experimental values, except for the $n = 2$ level, for which agreement is only slightly worse at 5.6%, unequivocally confirming our assignment of the optical transitions. It is worth noting that the $n = 4$ level is not confined to the dot, but is in the $\text{Al}_x\text{Ga}_{1-x}\text{As}$ layer bounded by the superlattice. Finally, we are now also able to determine the confinement energy of the hole ground state: this is simply the difference in energy between Peak 4 and Peak 5, taking into account the carbon acceptor binding energy, i.e. $1803 \text{ meV} - 1756 \text{ meV} - 30 \text{ meV} = 17 \text{ meV}$.

Having identified the PL peaks and determined the confinement energies in the system, we now go on to discuss the phonon bottleneck in this system. In Fig. 2(a) it is striking that Peak 4, associated with recombination from the highest energy state, $n = 4$, is the most intense, and that the intensity decreases with decreasing n . This is despite the fact that the data is taken at low temperature and the separation of adjacent PL peaks (the confined electron states) is between 16 and 41 meV, while the gap between the $n = 1$ and $n = 4$ levels is 88 meV, which corresponds to a thermal energy of 1000 K. Nevertheless, we suggest that the relative intensity of the peaks does reflect the occupation of the states, i.e. that at low temperature the $n = 4$ state has the highest occupancy, and $n = 1$ the lowest. Moreover, the laser excitation powers used in the experiments are very low ($\sim 10^{-5} \text{ Wcm}^{-2}$), so occupation of confined electrons states $n > 1$ cannot be the result of state filling. The occupancies of the energy levels are, thus, non-equilibrium. We attribute this to the phonon-bottleneck effect.

Fig. 2(a) also shows that at low temperature Peak 4 is a few hundred times more intense than Peak 5. Since both transitions involve the electrons in the $n = 4$ level, this difference in intensity implies that there are very few holes in the QD ground state. In the absence of holes (or with holes in a bound state with a well-defined energy) the phonon bottleneck is manifest, and the electrons

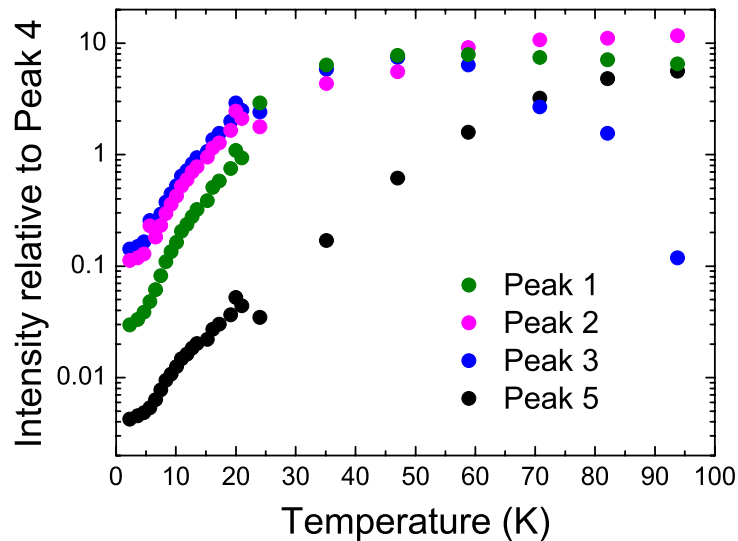


FIG. 4. Temperature dependence of the PL peak intensities relative to Peak 4. Raising the temperature thermalizes the holes, increasing the occupancy the quantum dot ground state and the relative intensity of Peak 5. This also turns off the phonon bottleneck, allowing electrons to relax to lower confined states, and increasing the relative intensity of Peaks 1 to 3.

are prevented from relaxing into lower energy states. To turn off the phonon bottleneck, we need to introduce free holes into the QDs, which we can do by increasing the temperature. Fig. 4, which plots the intensities of Peaks 1, 2, 3 and 5 relative to that of Peak 4, shows the effect of raising the temperature and removing the phonon bottleneck. It is interesting that the largest increase in relative intensity is for Peak 5 (by more than a factor of 1000). Since Peak 4 and Peak 5 share a common initial state for the electron, this reveals a massive increase in the number of holes in the QD ground state. The following picture of the hole dynamics in the sample thus emerges: At the lowest temperatures photo-excited holes are attracted to, and trapped by, negatively-charged (unoccupied) acceptors, such that confined electron to A^0 recombination dominates (note that after recombination the acceptors are unoccupied again). Increasing the temperature allows holes to thermalize out of the superlattice and $\text{Al}_x\text{Ga}_{1-x}\text{As}$, raising the occupancy of the confined hole states in the QDs. Given that the C acceptor binding energy is ~ 30 meV, it is reasonable to assume that increasing the temperature to 100 K does not significantly reduce the number of C acceptors in the dots that are occupied with holes. Hence, the 1000-fold increase in relative intensity of Peak 5 implies that the proportion of QDs with acceptors is a fraction of 1%. Indeed, the increase in intensity of Peak 5 is made even more remarkable when we consider what is happening to the electrons in the system: Introducing free holes into the QDs turns off the phonon bottleneck, allowing electrons to relax into the $n = 1$ to 3 levels, increasing the relative intensities of Peaks 1 to 3 by approximately a factor of 100. Finally, we note that intense PL is observed in this system all the way up to room temperature, although detailed identification of the transitions becomes difficult as features become thermally broadened and redistribution of the carriers makes transitions such as electron ground state to hole ground state optically active.³³

In summary, we have presented low-temperature photoluminescence measurements on highly uniform $\text{GaAs}/\text{Al}_x\text{Ga}_{1-x}\text{As}$ quantum dots for which recombination between electrons and holes bound to carbon acceptors is observed, allowing us to determine the energies of all the confined electron states in the system and the confinement energy of the hole ground state. The assignments of the energy levels are confirmed by effective mass calculations. The presence of carbon in the dots is shown to give rise to a dramatic demonstration of the phonon bottleneck.

This work was partly supported by the Engineering and Physical Sciences Research Council. The data in the figures for this manuscript are openly available from Lancaster University data archive at <http://dx.doi.org/10.17635/lancaster/researchdata/9>.

- ¹ J.H. Davies, *The physics of low-dimensional semiconductors* (Cambridge University Press, Cambridge, 1997).
- ² H. Benisty, C. M. Sotomayor-Torres, and C. Weisbuch, *Phys. Rev. B* **44**, 10945-10948 (1991).
- ³ J. Urayama, T. B. Norris, J. Singh, and P. Bhattacharya, *Phys. Rev. Lett.* **86**, 4930-4933 (2001).
- ⁴ R. Heitz, M. Veit, N. N. Ledentsov, A. Hoffmann, D. Bimberg, V. M. Ustinov, P. S. Kop'ev, and Zh. I. Alferov, *Phys. Rev. B* **56**, 10435-10444 (1997).
- ⁵ I. Vurgaftman and J. Singh, *Appl. Phys. Lett.* **64**, 232-234 (1994).
- ⁶ N. Koguchi and K. Ishige, *Jpn. J. Appl. Phys.* **32**, 2052-2058 (1993).
- ⁷ S. Huang, Z. Niu, Z. Fang, H. Ni, Z. Gong, and J. Xia, *Appl. Phys. Lett.* **89**, 031921 (2006).
- ⁸ C. Somaschini, S. Bietti, N. Koguchi, and S. Sanguinetti, *Nano Lett.* **9**, 3419-3424 (2009).
- ⁹ M. Jo, T. Mano, Y. Sakuma, and K. Sakoda, *Appl. Phys. Lett.* **100**, 212113 (2012).
- ¹⁰ K. Reyes, P. Smereka, D. Nothorn, J. M. Millunchick, S. Bietti, C. Somaschini, S. Sanguinetti, and C. Frigeri, *Phys. Rev. B* **87**, 165406 (2013).
- ¹¹ M. Jo, T. Mano, and K. Sakoda, *Appl. Phys. Express* **3**, 045502 (2010).
- ¹² K. Watanabe, N. Koguchi, and Y. Gotoh, *Jpn. J. Appl. Phys.* **39**, L79-L81 (2000).
- ¹³ M. Jo, G. Duan, T. Mano, and K. Sakoda, *Nanoscale Res. Lett.* **6**, 76 (2011).
- ¹⁴ C. H. Goo, W. S. Lau, T. C. Chong, L. S. Tan, and P. K. Chu, *Appl. Phys. Lett.* **68**, 841-843 (1996).
- ¹⁵ I. V. Kukushkin and V. B. Timofeev, *JETP Lett.* **43**, 387-390 (1986).
- ¹⁶ I. V. Kukushkin, K. von Klitzing, K. Ploog, and V. B. Timofeev, *Phys. Rev. B* **40**, 7788-7792 (1989).
- ¹⁷ I. V. Kukushkin and V. B. Timofeev, *Adv. Phys.* **45**, 147-242 (1996).
- ¹⁸ A. S. Plaut, I. V. Kukushkin, K. von Klitzing, and K. Ploog, *Phys. Rev. B* **42**, 5744-5750 (1990).
- ¹⁹ I. V. Kukushkin, K. von Klitzing, and K. Ploog, *Phys. Rev. B* **37**, 8509-8512 (1988).
- ²⁰ H. Buhmann, W. Joss, K. von Klitzing, I. V. Kukushkin, G. Martinez, A. S. Plaut, K. Ploog, and V. B. Timofeev, *Phys. Rev. Lett.* **65**, 1056-1059 (1990).
- ²¹ I. V. Kukushkin, R. J. Haug, K. von Klitzing, and K. Ploog, *Phys. Rev. Lett.* **72**, 736-739 (1994).
- ²² H. Buhmann, W. Joss, K. von Klitzing, I. V. Kukushkin, A. S. Plaut, G. Martinez, K. Ploog, and V. B. Timofeev, *Phys. Rev. Lett.* **66**, 926-929 (1991).
- ²³ I. V. Kukushkin, V. I. Fal'ko, R. J. Haug, K. von Klitzing, K. Eberl, and K. Totemayer, *Phys. Rev. Lett.* **72**, 3594-3597 (1994).
- ²⁴ R. Singh and G. Bester, *Phys. Rev. B* **85**, 205405 (2012).
- ²⁵ O. Madelung, *Semiconductors: Data Handbook* (Springer, New York, 2004).
- ²⁶ P. Atkinson, E. Zallo, and O. G. Schmidt, *J. Appl. Phys.* **112**, 054303 (2012).
- ²⁷ Ch. Heyn, A. Stemmann, M. Klingbeil, Ch. Strelow, T. Köppen, S. Mendach, and W. Hansen, *J. Crystal Growth* **323**, 263-266 (2011).
- ²⁸ C. Somaschini, S. Bietti, N. Koguchi, and S. Sanguinetti, *Nanotechnology* **22**, 185602 (2011).
- ²⁹ I. Vurgaftman, J. R. Meyer, and L. R. Ram-Mohan, *J. Appl. Phys.* **89**, 5815-5875 (2001).
- ³⁰ J. G. Keizer, J. Bocquel, P. M. Koenraad, T. Mano, T. Noda, and K. Sakoda, *Appl. Phys. Lett.* **96**, 062101 (2010).
- ³¹ We also performed calculations with a more realistic shape, but it hardly changed the results and required more parameters.
- ³² A. J. Robson, I. Grishin, R. J. Young, A. M. Sanchez, O. V. Kolosov, and M. Hayne, *ACS Appl. Mater. Interfaces* **5**, 3241-3245 (2013).
- ³³ The electron to heavy-hole ground state transition is expected at $1668 \text{ meV} + 30 \text{ meV} + 17 \text{ meV} = 1715 \text{ meV}$ at low temperature, which puts it in between Peaks 2 & 3.